Transmission Torque Analysis of Permanent Magnet Axial Eddy Current Couplings with Misalignment

Ao Wang, Shaoqing Zheng, Jian Wang

Abstract—**In order to study the output torque characteristics of permanent magnetic (PM) axial eddy current coupling under misaligned conditions. Firstly, the 3D structure model of PM axial eddy current coupling is established, and then various misalignment forms existing in PM axial eddy current coupling are analyzed. Finally, the magnetic induction intensity distribution, eddy current distribution and output torque under various misalignment forms are studied by finite element software. The results show that there are three forms of angular misalignment, radial misalignment and compound misalignment in PM axial eddy current coupling. The output torque increases as the angular angle increases and as the radial distance decreases, and the output torque operates stably in all three misalignment forms. The analysis results have a good guiding significance for the installation and operation of PM axial eddy current coupling.**

Index Terms—**permanent magnetic (PM), eddy current coupling, eddy current distribution, output torque, misalignment**

I. Introduction

PERMANENT magnetic (PM) eddy current coupling is a device that transfers torque from an input to an output. Compared with traditional couplings, PM eddy current coupling has the advantages of no friction, overload protection, soft start, due to the non-mechanical contact between the input rotor and the output rotor. It is widely popular in coal mining, marine, chemical industry, and other fields [1-3].

Due to the unique advantages of PM eddy current coupling, it has been widely studied by scholars around the world [4-9]. Cheng [10] established the output torque model of the magnetic coupler by using the equivalent magnetic circuit method and verified the accuracy of the model under the condition of a small gap and small speed difference by comparing it with the simulation results. Belguerras [11] proposed a high-temperature superconducting disc magnetic coupler that uses a cylindrical PM to wrap a flat high-temperature superconducting coil around a PM and proposed a two-dimensional analytical model. It is verified that the calculated values of the air gap magnetic field and electromagnetic torque are in good agreement with the simulated and experimental values by finite element and experiment. Wang [12] A three-dimensional layer model of the output torque of the magnetic coupler is established in the three-dimensional Cartesian coordinate system by using the vector magnetic potential method. The comparison with the simulation and test results verifies that the model has high accuracy under any circumstances. Aberoomand [13] optimized the analytical model of a double-sided PM eddy current coupler, established a steady-state model considering the geometric parameters and material properties of the coupler by using the equivalent magnetic circuit method, derived the torque-velocity curve from it, and optimized the dynamic processes such as the coupler by using genetic algorithm. Guo [14] based on considering the magnetic field interaction between adjacent eddy currents in the conductor layer, the output torque formula of the magnetic coupler is derived by using the equivalent magnetic circuit method and the ampere-loop theorem. By comparing with the simulation results, the accuracy of the model under large speed difference is verified. A limited number of Hall sensors were used to continuously reconstruct the distribution of the internal magnetic field in a short period, and the related parameters such as speed and torque were estimated [17]. The experimental results verified that the proposed method was good, and the relative errors of speed and torque estimation were about 4% and 6%, respectively. Wang [16] designed and manufactured a complex magnetic coupler, established a three-dimensional magnetic field distribution model to study the influence of structural parameters on the dynamic performance of the complex magnetic coupler, and optimized its structural parameters by using the improved response surface method. The optimization results can provide the theoretical and technical basis for the design of the complex magnetic coupler. Luo [15] proposed an online magnetic-thermal coupling model for real-time reconstruction of the magnetic-thermal coupling field in PM eddy current couplers. The effectiveness of the magnetic-thermal coupling model in the reconstruction of main magnetic field components, torque estimation, and temperature prediction was confirmed by comparison between the experiment and the model prediction. The above research mainly focuses on the magnetic field strength and output torque of PM eddy current coupling. However, PM eddy current coupling and conductor rotors often operate in

Manuscript received May 21, 2024; revised October 8, 2024.

Ao Wang is a PhD candidate in the School of Mechanical Engineering, Jiangsu University, Zhenjiang Jiangsu, 212013, China. (corresponding author to provide phone: 15551786981; email: wangao20220424@163.com).

Shaoqing Zheng is a PhD candidate in the School of Mechanical Engineering, Jiangsu University, Zhenjiang Jiangsu, 212013, China. (email: zsq2350594@126.com).

Jian Wang is a postgraduate student in the School of Mechanical Engineering, Jiangsu University, Zhenjiang Jiangsu, 212013, China. (email: chn_wangjian@163.com).

misalignment due to misalignment of the installation or the impact of vibration, high temperature, and shaft deflection during long-term operation. Therefore, it is necessary to study the magnetic field strength and output torque of PM eddy current coupling in misalignment.

In this paper, the PM axial eddy current coupling with six pairs of poles is taken as the research object. The magnetic induction intensity distribution, eddy current distribution, and output torque of the conductor sheet surface under three misalignment modes were simulated by finite element software. The results are compared with those in the case of full alignment, and the influence of three misalignment forms on the working state of PM axial eddy current coupling is analyzed.

II. Model Analysis

A. Structure of PM axial eddy current coupling

Fig. 1 shows the 3D structure of PM axial eddy current coupling. The input rotor comprises an input shaft, conductor back iron, and conductor sheet, in which the conductor sheet is made of copper. The output rotor consists of PM back iron, PM, and output shaft, where the material of PM is NdFeB, and the N pole and S pole PM are arranged alternately. The structural parameters and material properties of PM axial eddy current coupling are shown in Table 1.

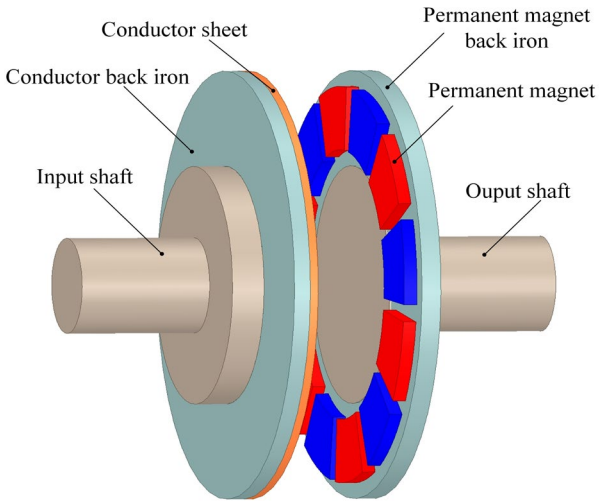

Fig. 1. 3D structure of PM axial eddy current coupling.

TABLE I
SPECIFICATIONS OF PM AXIAL EDDY CURRENT COUPLING

Parameter	Value
Number of PM pole pairs	6
Inner radius of the PMs	85 mm
Outer radius of the PMs	125 mm
Thickness of the PMs	8 mm
Inside radius of the conductor sheet	75 mm
Outside radius of the conductor sheet	135 mm
Thickness of the conductor sheet	5 mm
Thickness of the PM back iron	12 mm
Thickness of the conductor back iron	10 mm
Air gap length	8 mm
Angle of pole pitch	30°
Angle of pole-arc	25°
Permeability of vacuum	4π×10-7 H/m
Relative permeability of PMs	1.099
Relative permeability of back iron	2000
Coercive force of the PMs	−868 kA/m
Conductivity of the conductor sheet	5.7×10^7 S/m

B. Analytical Model for Misalignment

PM axial eddy current coupling due to manufacturing errors, installation errors, stress deformation, and thermal deformation caused by high temperature in the working process, the complete alignment between input shaft and output shaft cannot be guaranteed. Fig. 2 shows the misalignment forms of PM axial eddy current coupling, which are divided into angular misalignment, radial misalignment, and compound misalignment. Angular misalignment is when there is a certain inclination between the input rotor and the output rotor, and the centers of the two rotors coincide radially. Radial misalignment means that the input rotor axis does not coincide with the output rotor axis and that the two axes are parallel. Compound misalignment means that there is a certain inclination between the input rotor and the output rotor, and the centers of the two rotors do not coincide in radial direction.

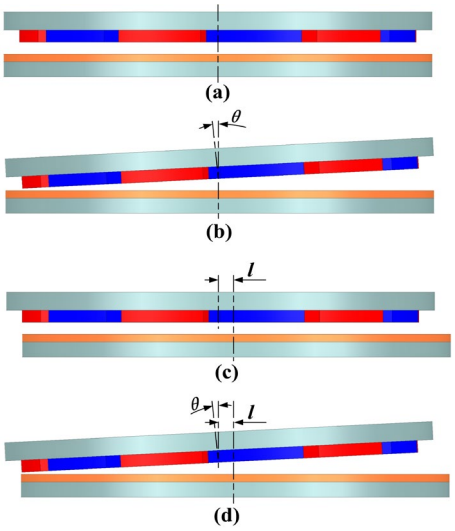

Fig. 2. Forms of misalignment. (a) No misalignment, (b) Angular misalignment, (c) Radial misalignment, (d) Compound misalignment.

III. Results and Discussion

Taking the structure of PM axial eddy current coupling as shown in Fig. 1 and the parameters in Table 1 as research objects, finite element software is used to calculate the magnetic field distribution, eddy current distribution, and output torque on the surface of the conductor sheet. The speed difference is set to 100 rpm, the angle misalignment inclination is 1°, 2° and 3° respectively, the radial misalignment intermediate distance is 4 mm, 8 mm, and 12 mm respectively, and the compound misalignment inclination and distance are 1° 4 mm, 3° 4 mm, 1° 12 mm, and 3° 12 mm respectively.

A. Angular Misalignment

Fig. 3 shows the magnetic induction intensity distribution of the surface of the conductor sheet at different inclination angles. It can be seen from Fig. 3 that the magnetic induction intensity is higher at the corresponding PM center and lower around the corresponding PM. As the inclination increases, the magnetic induction intensity on one side of the conductor sheet gradually increases, while the other side gradually decreases. This is because the greater the inclination, the smaller the distance between PM and the conductor sheet on one side, the larger the distance on the other side, the higher

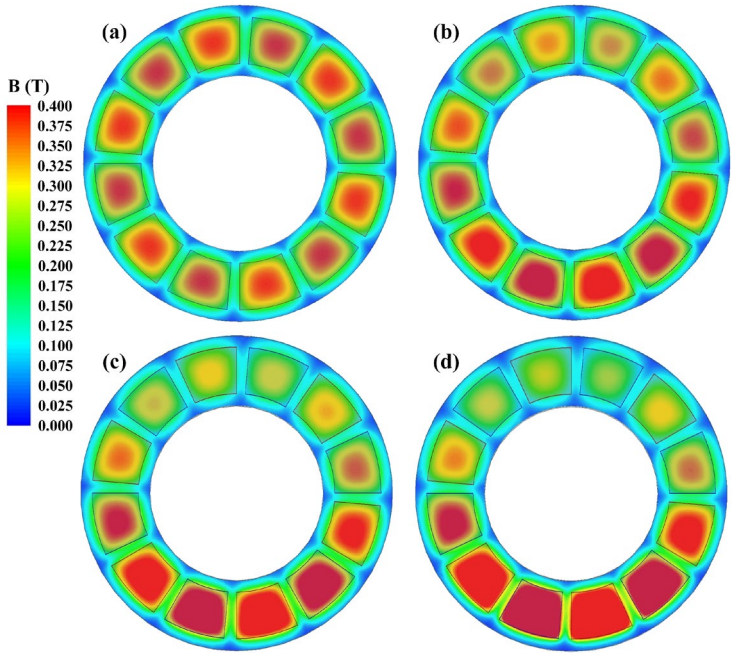

Fig. 3. Angular misalignment of magnetic induction intensity distribution. (a) 0°, (b) 1°, (c) 2°, (d) 3°.

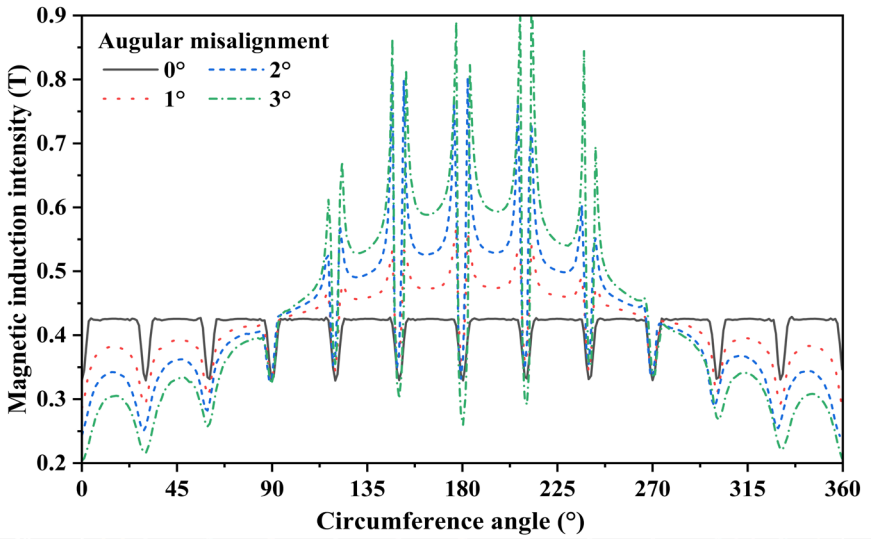

Fig. 4. Angular misalignment of magnetic induction intensity value.

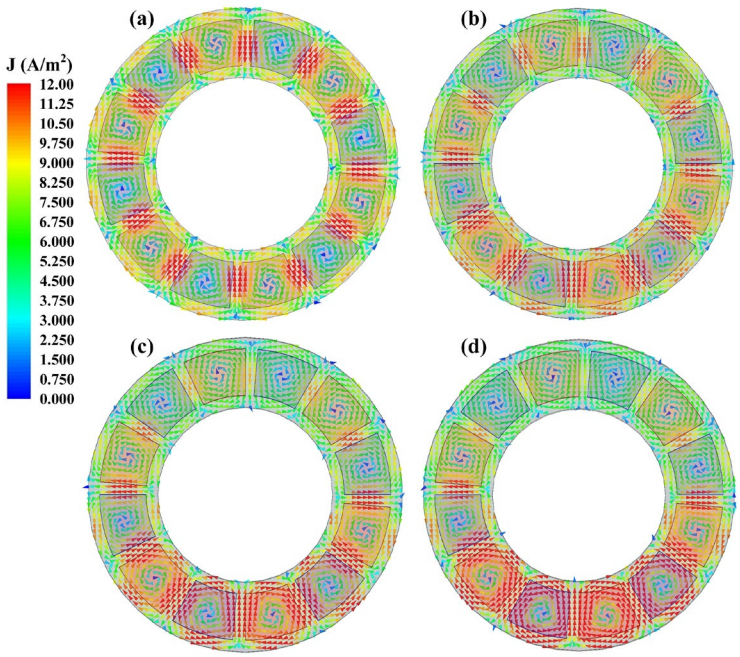

Fig. 5. Angular misalignment of eddy current distribution. (a) 0°, (b) 1°, (c) 2°, (d) 3°.

the magnetic induction intensity on the side with the smaller distance, and the lower the magnetic induction intensity on the side with the larger distance.

Fig. 4 shows the magnetic induction intensity of a circle on the surface of the conductor sheet with the spindle center as the center of the circle 105 mm (the middle value of the inner and outer diameters of the conductor sheet) as the radius under different angular misalignments. When no angular deflection occurs, the magnetic induction intensity on the surface of the conductor sheet changes periodically, and the magnetic induction intensity corresponding to the center of the PM is the largest, with a maximum value of 0.425 T. The magnetic induction intensity changes dramatically with the increase of the angular misalignment value. The magnetic induction value decreases away from the PM. The magnetic induction intensity near the PM increases, and the increase amplitude increases with the increase of the deflection angle, and the maximum can reach 0.9 T.

Fig. 5 shows the eddy current distribution of the surface of the conductor sheet at different inclination angles. It can be seen from fig. 5 that the center of the eddy current loop corresponds to the PM center and the maximum eddy current distribution corresponds to the region between adjacent PM. As the inclination increases, the eddy current on one side of the conductor sheet gradually increases and the other side gradually decreases. The reason is the same as the magnetic induction intensity in fig. 3. The greater the inclination, the smaller the distance between PM and the conductor sheet on one side, the larger the distance on the other side, and the higher eddy current on the side with the smaller distance. The eddy current is lower on the side with a larger distance.

Fig. 6 shows the output torque curve of PM axial eddy current coupling at different inclination angles. It can be seen from fig. 6 that the output torque gradually increases from 0-20 ms and becomes stable after 20 ms. This indicates that angular misalignment does not change the stability of the output torque of the PM axial eddy current coupling. With the increase of inclination angle, the output torque of PM axial eddy current coupling gradually increases, and the higher the inclination angle, the greater the increased range. This is because in the case of a large inclination angle, there is a minimal distance between PM and the conductor sheet, and the magnetic induction intensity and eddy current on the surface of the conductor sheet at a small distance is huge, and their output torque increases.

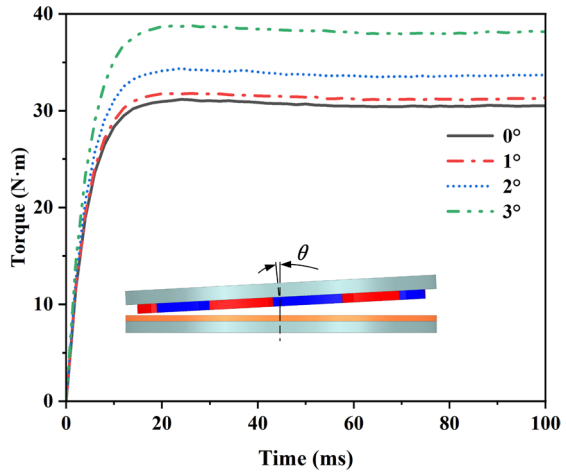

Fig. 6. Angular misalignment of output torque.

B. Radial Misalignment

Fig. 7 shows the magnetic induction intensity distribution of the surface of the conductor sheet at different radial distances. It can be seen from fig. 7 that the magnetic induction intensity of the surface of the conductor sheet is larger in the regions corresponding to the PM center, while the regions corresponding to the periphery of the PM are smaller. The regions with large magnetic induction intensity on the surface of the conductor sheet change with the change of radial distance, but the magnetic induction intensity does not change significantly.

Fig. 8 shows the magnetic induction intensity of a circle on the surface of the conductor sheet with the spindle center as the center of the circle 105 mm (the middle value of the inner and outer diameters of the conductor sheet) as the radius under different radial misalignments. Under different radial deflection distances, the magnetic induction intensity presents a periodic distribution. and the magnetic induction intensity corresponding to the center of the PM is the largest. With the increase of the radial deflection distance, the magnetic induction intensity decreases gradually, but the decreasing range is small. When the radial deflection distance is 0 mm, the maximum magnetic induction intensity is 0.425 T. When the radial deflection distance is 12 mm, the maximum magnetic induction intensity is 0.42 T. Radial misalignment has little effect on magnetic induction on the surface of the conductor sheet.

Fig. 9 shows the eddy current distribution of the surface of the conductor sheet at different radial distances. It can be seen from fig. 9 that the center of the eddy current loop corresponds to the PM center, and the maximum eddy current distribution corresponds to the region between adjacent PMs. The center of the vortex circuit changes with the change in radial distance, but the vortex size does not change significantly.

Fig. 10 shows the PM axial eddy current coupling output torque curve at different radial distances. It can be seen from fig. 10 that the output torque gradually increases from 0-20ms and becomes stable after 20 ms. This indicates that radial misalignment does not change the stability of the PM axial eddy current coupling output torque. With the increase of radial distance, the output torque of PM axial eddy current coupling gradually decreases, and the greater the radial distance, the greater the reduction range.

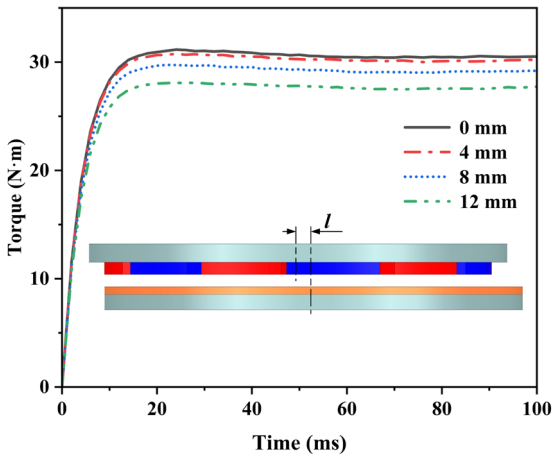

Fig. 10. Radial misalignment of output torque.

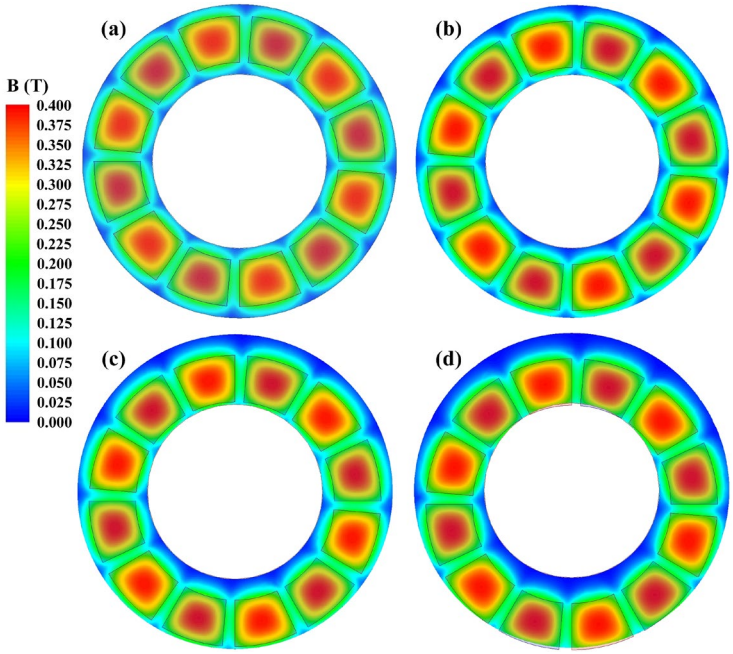

Fig. 7. Radial misalignment of magnetic induction intensity distribution. (a) 0 mm, (b) 4 mm, (c) 8 mm, (d) 12 mm.

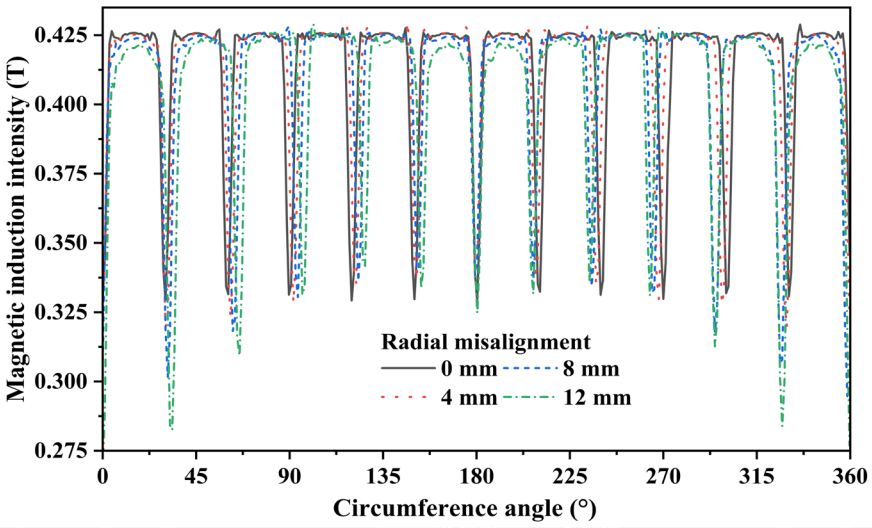

Fig. 8. Radial misalignment of magnetic induction intensity value.

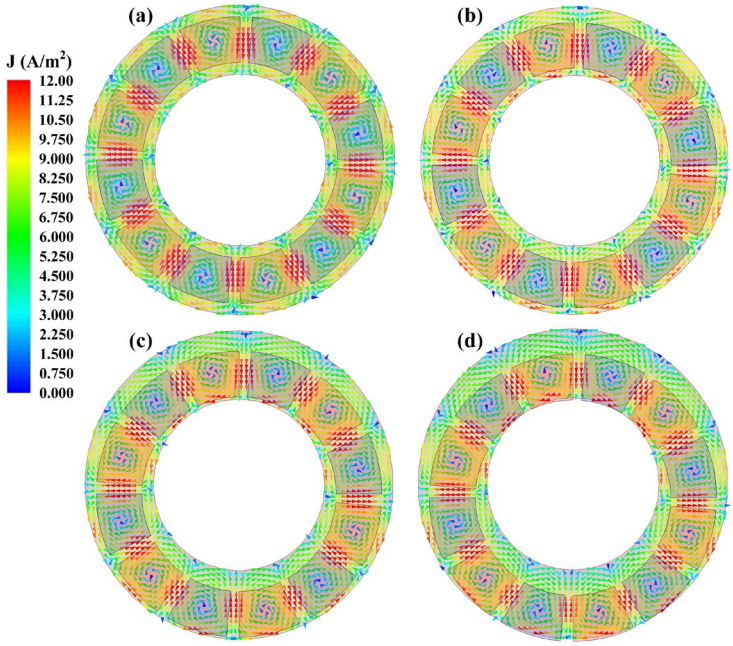

Fig. 9. Radial misalignment of eddy current distribution. (a) 0 mm, (b) 4 mm, (c) 8 mm, (d) 12 mm.

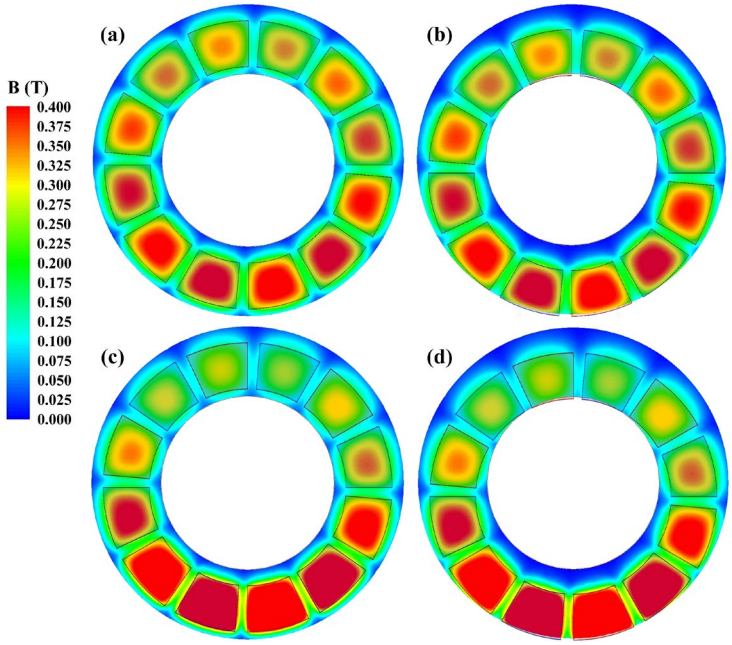

Fig. 11. Compound misalignment of magnetic induction intensity distribution. (a) 1°, 4 mm, (b) 1°, 12 mm, (c) 3°, 4 mm, (d) 3°, 12 mm.

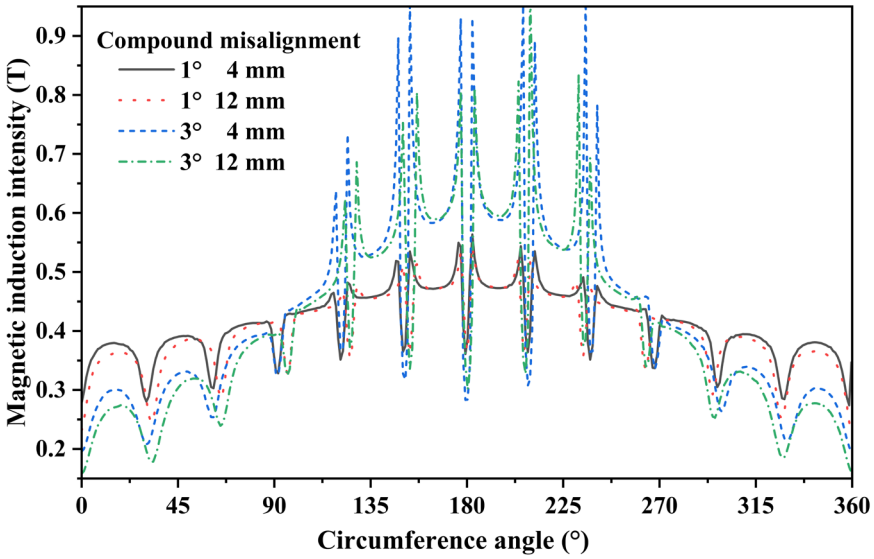

Fig. 12. Compound misalignment of magnetic induction intensity value.

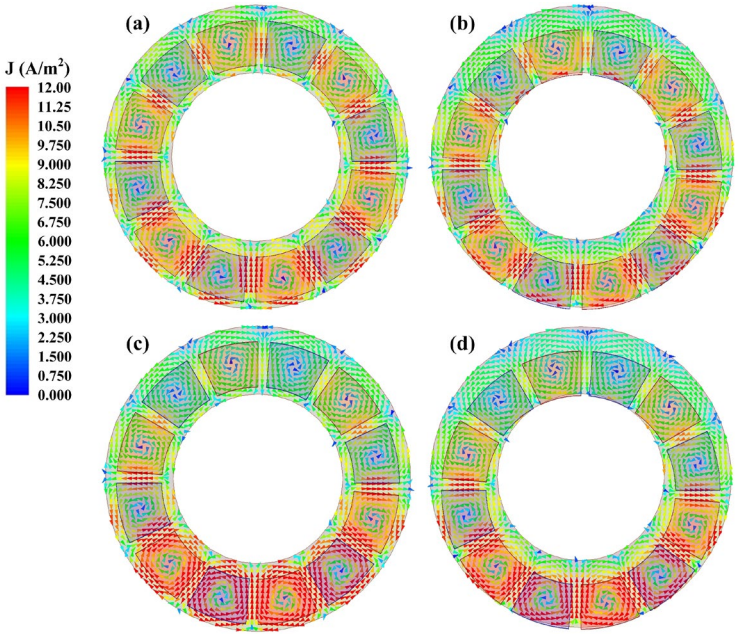

Fig. 13. Compound misalignment of eddy current distribution. (a) 1°, 4 mm, (b) 1°, 12 mm, (c) 3°, 4 mm, (d) 3°, 12 mm.

This is due to the shift of magnetic induction intensity and eddy current position on the surface of the conductor sheet as the radial distance increases. The total magnetic induction intensity and eddy current are reduced. In addition, when the radial distance is larger, the larger magnetic induction intensity and eddy current on the surface of the conductor sheet are lost due to the position deviation. The total magnetic induction intensity and eddy current are reduced.

C. Compound Misalignment

Fig. 11 shows the magnetic induction intensity distribution of the surface of the conductor sheet at different inclination angles and radial distances. It can be seen from fig. 11 that the magnetic induction intensity on the surface of the conductor sheet is relatively large in the regions corresponding to the PM center, and relatively small in the regions corresponding to the periphery of the PM. Under the same inclination angle, the location of the large magnetic induction intensity region on the conductor sheet changes with the change of the radial distance, but the magnitude of the magnetic induction intensity does not change. Under the same radial distance, the magnetic induction intensity on the surface of the conductor sheet changes with the change of the inclination angle. The larger the inclination, the greater the magnetic induction intensity on one side of the conductor sheet surface and the smaller the magnetic induction intensity on the other side.

Fig. 12 shows the magnetic induction intensity of a circle on the surface of the conductor sheet with the spindle center as the center of the circle 105 mm (the middle value of the inner and outer diameters of the conductor sheet) as the radius under different compound misalignments. The magnetic induction intensity changes dramatically with the increase of the angular misalignment value. The magnetic induction value decreases away from the PM. The magnetic induction intensity near the PM increases, and the increased amplitude increases with the increase of the deflection angle, and the maximum can reach 0.9 T. With the increase of the radial deflection distance, the magnetic induction intensity decreases gradually, but the decreasing range is small. Radial misalignment has little effect on magnetic induction on the surface of the conductor sheet. Angular misalignment is the main factor affecting magnetic induction on the surface of a conductor sheet.

Fig. 13 shows the eddy current distribution of the surface of the conductor sheet at different inclination angles and radial distances. It can be seen from fig. 13 that the center of the eddy current loop corresponds to the PM center, and the maximum eddy current distribution corresponds to the region between adjacent PMs. With the same inclination angle, the center and the maximum distribution position of the eddy current change with the change of radial distance, and the eddy current size does not change with the change of radial distance. At the same radial distance, the eddy current on the surface of the conductor sheet changes with the change of inclination. The larger the inclination, the larger the eddy current on one side of the conductor sheet surface and the smaller the eddy current on the other side.

Fig. 14 shows the PM axial eddy current coupling output torque curve at different inclination angles and radial distances. It can be seen from fig. 14 that the output torque gradually increases from 0-20 ms and reaches stability after 20 ms. At the same inclination angle, when the radial distance increases, the output torque of PM axial eddy current coupling decreases. With the same radial distance, the PM axial eddy current coupling output torque increases when the inclination angle increases. This is the same phenomenon shown in fig. 6 and 10, and the principle is the same. The above phenomena can indicate that angular misalignment, radial misalignment, and compound misalignment only change the output torque size, but not the output torque stability. PM axial eddy current coupling can operate normally.

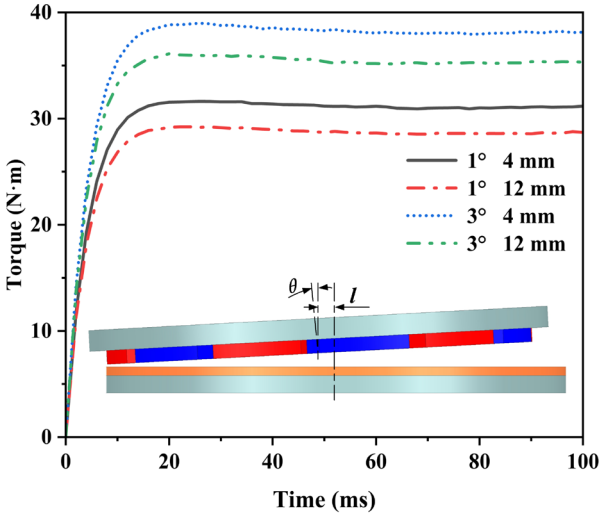

Fig. 14. Compound misalignment of output torque.

Fig. 15 shows the variation law of output torque under angular misalignment, radial misalignment and compound misalignment. With the increase of radial misalignment Angle, the output torque decreases gradually. As the Angle of misalignment increases, the output torque increases, and the range of improvement increases gradually. The angular misalignment has great influence on the output torque, which is the main factor affecting the output torque.

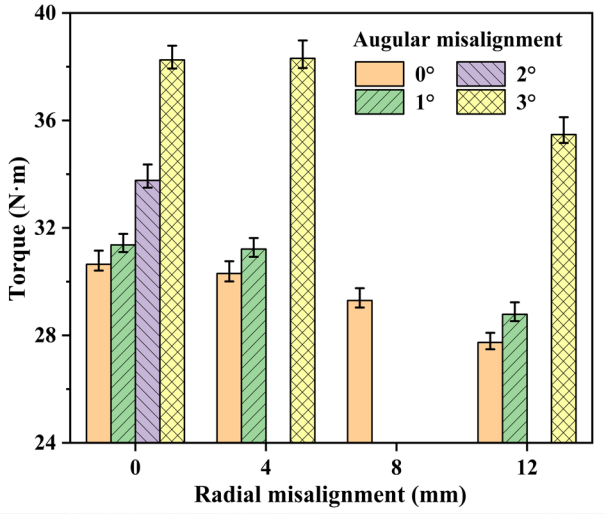

Fig. 15. Misalignment of output torque.

IV. Conclusion

Taking PM axial eddy current coupling as the research object. Using finite element software to study its angular misalignment, radial misalignment, and compound

misalignment magnetic induction intensity distribution, eddy current distribution, and output torque, the results are as follows.

1. In angular misalignment, the range of magnetic induction intensity and eddy current gradually increases with the increase of inclination angle, and the output torque gradually increases.

2. In radial misalignment, with the increase of radial distance, the distribution position of magnetic induction intensity and eddy current change, but the size does not change, and the output torque gradually decreases.

3. In compound misalignment, radial distance remains unchanged, the range of magnetic induction intensity and eddy current and output torque increase with the increase of inclination angle, and the inclination angle remains unchanged. The distribution positions of magnetic induction intensity and eddy current change with the change of radial distance, and the output torque decreases with the increase of radial distance.

4. In angular misalignment, radial misalignment, and compound misalignment under three working conditions PM axial eddy current coupling output torque is stable. PM axial eddy current coupling can operate normally.

REFERENCES

[1] Kais Atallah and Jiabin Wang, "A Brushless Permanent Magnet Machine with Integrated Differential," IEEE Transaction on Magnetics, vol. 47, no. 10, pp4246– 4249, 2011.

[2] Xin Dai, Qinghua Liang, Jiayong Cao, Yongjun Long, Jinqiu Mo, and Shigang Wang, "Analytical Modeling of Axial-flux Permanent Magnet Eddy Current Couplings with a Slotted Conductor Topology," IEEE Transactions on Magnetics, vol. 52, no. 2, pp8000315, 2016.

[3] Lezhi Ye, Desheng Li, Yuanjing Ma, and Bingfeng Jiao, "Design and Performance of a Water-cooled Permanent Magnet Retarder for Heavy Vehicles," IEEE Transactions on Energy Conversion, vol. 26, no. 3, pp953–958, 2011.

[4] George Buzuzi, Mangwiro Magodora, Martin T Kudinha, William M Manamela, and Mobele H Mambo, "Steady MHD Williamson Nanofluid Flow Past an Inclined Stretching Sheet in the Presence of Heat Generation, Chemical Reaction and Aligned Magnetic Field," IAENG International Journal of Applied Mathematics, vol. 54, no. 6, pp1125-1135, 2024.

[5] Lirong Wang, Sayang Mohd Deni, and Zalina Zahid, "A LogTV Nonconvex Regularization Model for Magnetic Resonance Imaging," Engineering Letters, vol. 31, no. 2, pp702-711, 2023.

[6] Nityanand P. Pai, Devaki B., Sampath Kumar V. S. and Pareekshith G. Bhat, "Analysis of Magnetic Effect on UCM Fluid Flow between a Stationary and a Moving Plate," Engineering Letters, vol. 32, no. 4, pp792-799, 2024.

[7] Di Huang, Binbin Sun, Tianqi Gu, Zhenwei Wang, Tiezhu Zhang and Yang Wang, "Design and Performance Analysis of Magnetic Bearings for Vehicle High-speed Flywheel Battery," Engineering Letters, vol. 31, no. 4, pp1691-1699, 2023.

[8] Md. Abdul Rawoof Sayeed, and Mohammed Majid Ali, "Entropy Generation during Cellular Magnetoconvection," Engineering Letters, vol. 30, no. 2, pp392-398, 2022.

[9] George Buzuzi, "Unsteady MHD Casson Fluid Flow Past an Inclined Surface Subjected to Variable Magnetic Field, Heat Generation and Effective Prandtl Number," Engineering Letters, vol. 31, no. 2, pp627-639, 2023.

[10] Xikang Cheng, Wei Liu, Yang Zhang, Sitong Liu, and Weiqi Luo, "A Concise Transmitted Torque Calculation Method for Pre-Design of Axial Permanent Magnetic Coupler," IEEE Transactions on Energy Conversion, vol. 35, no. 2, pp938–947, 2020.

[11] L. Belguerras, S. Mezani, and T. Lubin, "Analytical Modeling of an Axial Field Magnetic Coupler with Cylindrical Magnets," IEEE Transaction on Magnetics, vol. 57, no. 2, pp1-5, 2021.

[12] Jian Wang, "A Generic 3-D Analytical Model of Permanent Magnet Eddy-current Couplings Using a Magnetic Vector Potential Formulation," IEEE Transactions on Industrial Electronics, vol. 69, no. 1, pp663-672, 2022.

[13] Vahid Aberoomand, Mojtaba Mirsalim, and Rasul Fesharakifard, "Design Optimization of Double-Sided Permanent-Magnet Axial Eddy-Current Couplers for Use in Dynamic Applications," IEEE Transactions on Energy Conversion, vol. 34, no. 2, pp909–920, 2019.

[14] Benzhen Guo, Desheng Li, Jiarui Shi, and Zhiwei Gao, "A Performance Prediction Model for Permanent Magnet Eddy-current Couplings Based on the Air-gap Magnetic Field Distribution," IEEE Transaction on Magnetics, vol. 58, no. 5, pp1–9, 2022.

[15] Weiqi Luo, Wei Liu, Jiarui Zhang, and Yang Zhang, "Online Magneto-Thermal Coupled Model of PMECCs Using Measured Boundaries," IEEE Transactions on Industrial Electronics, vol. 71, no. 4, pp4162–4170, 2024.

[16] Shuang Wang, Kun Hu, and Deyang Li, "Optimal Design Method for the Structural Parameters of Hybrid Magnetic Coupler," Journal of Mechanical Sciences and Technology, vol. 33, no. 1, pp173–182, 2019.

[17] Weiqi Luo, Wei Liu, Xikang Cheng, Yang Zhang, and Zhenyuan Jia, "In Situ Magnetic Field Reconstruction and Torque Estimation for PMECCs," IEEE Transactions on Industrial Electronics, vol. 69, no. 12, pp13535–13543, 2022.

Ao Wang received the M.S. degree in mechanical engineering from Anhui Polytechnic University, Wuhu, Anhui Province, in 2023. He is currently working toward the doctorate degree with the Jiangsu University of Technology, Zhenjiang, China. His main research interests include the simulation, design, and optimization of PM eddy current coupling.

Shaoqing Zheng received the M.S. degree in mechanical engineering from Xiangtan University, Xiangtan, Hunan Province, in 2012. He is currently working toward the doctorate degree with the Jiangsu University of Technology, Zhenjiang, China. His research focusing on electromagnetic-thermal coupling calculation of PM eddy current coupling.

Jian Wang received the B.S. degree in mechanical engineering from Lanzhou University of Technology, Lanzhou, Gansu Province. He is currently working toward the M.S. degree with the Jiangsu University of Technology, Zhenjiang, China. His research focusing on finite element model of PM eddy current coupling.